

Confidential Prompting: Protecting User Prompts from Cloud LLM Providers

In Gim^{*}, *Caihua Li*^{*}, *Lin Zhong*
 Department of Computer Science
 Yale University

{in.gim, caihua.li, lin.zhong}@yale.edu

^{*} Both authors contributed equally

Abstract

Our work tackles the challenge of securing user inputs in cloud-hosted large language model (LLM) serving while ensuring model confidentiality, output invariance, and compute efficiency. We introduce *Secure Partitioned Decoding (SPD)*, which uses confidential computing to confine user prompts to a trusted execution environment (TEE), namely a confidential virtual machine (CVM), while allowing service providers to generate tokens efficiently. We also introduce a novel cryptographic method, *Prompt Obfuscation (PO)*, to ensure robustness against reconstruction attacks on SPD. We demonstrate our approach preserves both prompt confidentiality and LLM serving efficiency. Our solution enables privacy-preserving cloud LLM serving that handles sensitive prompts, such as clinical records, financial data, and personal information.

1 Introduction

Large language models (LLMs) are often hosted on cloud platforms, which introduces privacy concerns as prompts can include sensitive data, ranging from personal communications to health information. Not surprisingly, many IT, financial and healthcare industries, wary of information breaches, restrict the usage of cloud LLM at work [17, 46]. Privacy concerns also subject cloud-hosted LLM services to regulations like GDPR and HIPAA [15, 32] and, as a result, hamper their adoption. Cloud-hosted LLM services further raise intellectual property (IP) concerns because prompts are increasingly recognized as IPs, with emerging marketplaces for them. Both privacy and IP concerns underscore the importance of safeguarding prompt confidentiality in cloud environments.

This paper aims at *confidential prompting* in cloud-hosted LLM services, which secures the confidentiality of user prompts while achieving another three crucial goals for commercial LLM service: model confidentiality, output invariance, and compute efficiency. (i) *Model confidentiality* ensures the LLM weights are kept secret from users. (ii) *Output invariance* guarantees the output of the LLM service remains the

same regardless of whether confidentiality measures are applied, ensuring the utility and reliability of the service. (iii) *Compute efficiency* requires the introduction of confidentiality measures does not significantly increase the service cost.

We assume the users and the cloud LLM providers are mutually untrusted and potentially seek to uncover each other’s secrets, namely user prompts and LLM weights. In particular for the cloud LLM providers, we consider two variants of Honest-but-Curious (HBC) threat model, which are HBC without or with unlimited computational resources. In both scenarios, the service providers adhere strictly to the prescribed computation steps for LLM inference; however, they also endeavor to extract user secrets with various resource budgets. Our approach provides different security guarantees over user prompt confidentiality under different HBC variants, specifically securing the entire prompts or sensitive segments in the prompts such as Personal Identifiable Information (PII).

As we present in §2.2 and §2.4, none of existing solutions achieve all of our goals under the same threat model. For example, techniques like edge inference [30] protect input by processing them locally, which do not work for large models hosted on cloud and require sharing LLM weights with the users, undermining model confidentiality. Differentially private in-context learning (DP-ICL) [54, 59] and data anonymization [10, 24, 52, 60], alter the output, thus violating output invariance. Although fully homomorphic encryption (FHE) [19, 22] preserves both model confidentiality and output invariance, its extensive computational demands restrict its feasibility for LLMs. More recently, Confidential Computing (CC) [8] has emerged as a promising approach to secure cloud-based DNN [26, 47, 49], particularly through the use of confidential virtual machines (CVMs) with GPU support. Although CVMs ensure output invariance, their naive applications either demand complete trust in the LLM provider or prove impractical for LLM serving. This impracticality raises due to the lack of batch parallelism and the large memory footprint of LLMs in user CVMs, which limits the scalability.

This work presents a new approach to confidential prompting that uses CVMs in an efficient and scalable manner, illus-

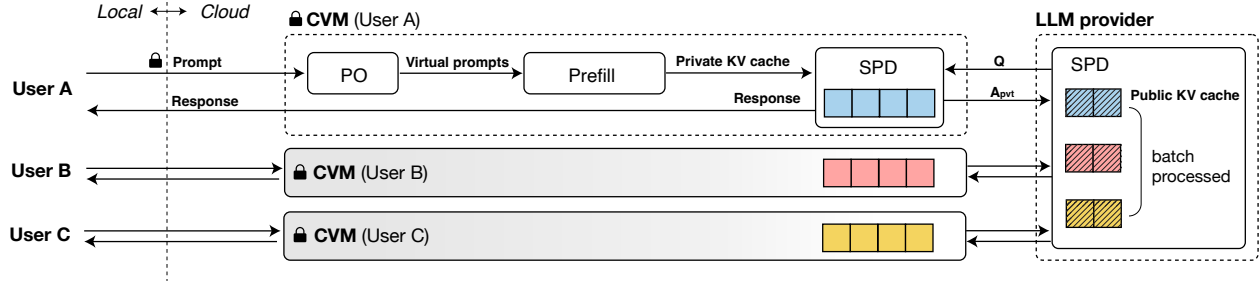


Figure 1: **Overview of Confidential Prompting by OSPD.** A user and its CVM collaborate to protect the user’s prompt from the cloud LLM provider by applying Secure Partitioned Decoding (SPD) and Prompt Obfuscation (PO). The user sends its encrypted prompt to its CVM hosted in the cloud. Then virtual prompts and private KV cache are prepared within the CVM during the prefill phase, while SPD involves both the CVM and the cloud LLM provider during the decode phase.

trated by Figure 1. Our key insight is that the delivery of LLM involves two distinct phases: prefill and decode, and the latter dominates computational use. Our approach, called *Obfuscated Secure Partitioned Decoding (OSPD)*, performs prefill inside per-user CVMs and keeps the resulting KV attention states (called private KV cache) there, as prefill requires the plaintext prompt and the private KV cache can be used to extract the prompt. OSPD then performs decode mostly outside the CVMs, without disclosing the private KV cache, using a technique called *Secure Partitioned Decoding (SPD)* (§4).

SPD formulates token generation (decode) as a secure two-party computation with one party being the CVM and the other the cloud LLM provider. In other words, we partition the attention score computation into two parts: the private and the public attention scores (A_{pvt} and A_{pub}), which are computed by the two parties respectively. During the decode, the CVM uses the private KV cache that is already precomputed in prefill to compute A_{pvt} . It does not require the LLM weights for computing A_{pvt} , thereby reducing the memory footprint of the CVM in decode. On the other hand, the cloud LLM providers compute the A_{pub} , merges it with A_{pvt} received from the CVM to generate new tokens, and then maintains the public KV cache for these newly generated tokens.

SPD secures the entire user prompt when assuming the attackers are HBC without unlimited computational resources. The user prompt is secure as the CVM exposes only the A_{pvt} , which does not expose the prompts or the private KV cache. SPD is also efficient because the service providers can batch process the public KV cache for multiple users in parallel, and the CVM does not retain LLM weights in decode, thereby remaining small footprint. Finally, SPD ensures output invariance as the attention score decomposition is lossless (§4.2).

However, SPD leaves three unsolved challenges. First, SPD is vulnerable to (semi) black-box reconstruction attacks, which approximate the prompt with public information to get user secrets if an attacker has unlimited computational resources. Second, SPD does not protect the LLM responses, unlike the naive CVM approaches that process completely within the CVM (§2.2.2). It is worth noting that, attempts

to uncover a prompt with its response is actually a kind of reconstruction attack. Details are in §4.3. Lastly, prefill requires LLM weights within the CVM and as a result, may jeopardize model confidentiality. OSPD mitigates the first two challenges with *Prompt Obfuscation (PO)* (§5) and solve the last challenge with control over the cloud infrastructure.

PO is a novel cryptographic method inspired by *chaffing and winnowing* (§2.3). To protect sensitive segments in a prompt, such as Personal Identifiable Information (PII), the CVM generates fake n-grams that appear as authentic as the original segments in the prompt. The CVM uses these fake n-grams to create λ *virtual prompts* and then process the $\lambda + 1$ prompts with prefill and SPD in parallel. In other words, the service providers learn nothing about the authentic and the virtual prompts or their private KV cache, except receiving $(\lambda + 1)$ private attention scores in a batch. Only the user and its CVM know which prompt (and response) is authentic.

PO mitigates the first two unsolved challenges left by SPD instead of offering absolute security. PO obfuscates the cloud LLM providers, but the latter may still succeed in guessing the authentic prompt (and response) with probability of $\epsilon + 1/(\lambda + 1)$, where ϵ is an error bound parameter used in sampling fake n-grams (§5.1). We offer a security analysis of PO in §5.2.

SPD and PO are complementary in two ways. On one hand, PO obfuscates the providers and offers a certain level of protection against reconstruction attacks. This minimizes the risk of leaking sensitive information in user prompts, while allowing SPD to offload majority of computation to out of CVMs. In other words, PO allows SPD to trade efficiency and scalability with minimal risk compared to naive CVM approaches. On the other hand, like many existing obfuscation methods, a knowledgeable attacker with more statistical information over the prompts has higher probability to break PO’s protection. However, SPD adds computational cost for the attacker to collect such statistical information and reduces its confidence in the collected data. Even if the attacker performs reconstruction attacks with unlimited computational resources, it hardly learns the exact plaintext prompts.

As for model confidentiality, OSPD addresses it by allow-

ing the cloud provider to check the integrity of the transferred output tokens, ensuring that the malicious client cannot exfiltrate LLM weights by sending arbitrary bytes. The cloud provider can also limit the outbound traffic to only what is necessary to transmit the generated tokens (§4.1).

In §6, we report an implementation of OSPD (SPD+PO) using PyTorch. In §7 we evaluate our prototype on NVIDIA H100 GPU with CC enabled, compared with two naive CVM approaches (§2.2.2). We show that OSPD scales well to the number of concurrent users and achieves $5\times$ better latency than the naive CVM approach that defends against cloud LLM providers. We conclude our work in §8 and discuss its limitations in §A.4, such as how to achieve stronger protection. We believe that cloud LLM serving that is both privacy-preserving and efficient is important and timely. Our work marks the first step towards utilizing confidential computing for secure LLM serving, and we hope it will spark further discussion on confidential prompting and methods offering stronger protection. The source code for OSPD can be found at github.com/yale-sys/confidential-prompting.

2 Background and Related Work

We next provide a succinct background about related techniques.

2.1 LLM Inference with KV cache

2.1.1 LLM Inference

We consider GPT-style LLMs [1, 7, 45, 55], which are trained to predict the distribution of the next token, x_{n+1} , given a sequence of tokens x_1, \dots, x_n , known as causal language modeling. This prediction process uses the Transformer architecture [56], which consists of multiple self-attention layers. For a sequence of length n , represented as $X \in \mathbb{R}^{n \times d}$, the Transformer produces an output sequence $Y \in \mathbb{R}^{n \times d}$, where d is the hidden dimension size. The self-attention mechanism, a core component of the Transformer, requires five matrix multiplications. First, the model computes matrices $Q = XW_Q$, $K = XW_K$, and $V = XW_V$, where W_Q, W_K , and $W_V \in \mathbb{R}^{d \times d}$ are trainable weight matrices. Next, the output is calculated as $Y = \sigma(QK^T)V \in \mathbb{R}^{n \times d}$, where $\sigma(\cdot)$ denotes the softmax function. The output becomes an input to the next layer. The LLM samples the next token x_{n+1} from the distribution and appends it to the token sequence, iteratively until some termination condition is met, so called autoregressive token generation.

2.1.2 KV Cache

The KV cache mechanism [18, 41, 44, 53] is a technique frequently used to improve LLM inference efficiency. This mechanism leverages the causal nature of LLMs: when predicting

a token x_i within a token sequence, the attention computation only considers preceding tokens, x_1, \dots, x_{i-1} , rather than any tokens that follow. Consequently, instead of recalculating attention for all tokens at each generation step, the LLM inference engine “caches” previously computed attention states and reuses them for subsequent inferences. Since the reusable attention states consist of the K and V matrices for each token, this technique is referred to as KV caching.

2.2 Confidential Computing and Inferencing

2.2.1 Confidential Computing

Confidential computing protects *data in use*, complementing traditional security measures such as encryption that protect *data at rest* and *data in transit*. The most common approach to confidential computing is to use trusted execution environments (TEEs), such as enclaves and confidential virtual machines (CVMs), which are provided by hardware features like AMD SEV [3] and Intel TDX [23]. These environments isolate sensitive data and code. Thanks to their strong isolation capabilities, hardware-based TEEs ensure even privileged entities such as the OS and hypervisor cannot access the data being processed. In addition to isolation, most hardware-based TEEs also provide runtime encryption and remote attestation. Runtime encryption guarantees all code and data within a CVM (or enclave) are encrypted in memory, offering an additional layer of protection. Remote attestation allows users to verify the integrity of a remote CVM (or enclave) running in the cloud before transmitting any sensitive data. Originally exclusive to CPUs, confidential computing is now supported by the latest GPUs as well, such as the NVIDIA H100 [40]. Many cloud providers offer confidential computing as a service, primarily through the use of CVMs [49]. Unlike regular VMs, which can share memory for read-only data such as LLM weights, CVMs do not share memory, to ensure confidential data remains securely isolated and encrypted. In this work, we use the terms TEE and CVM interchangeably.

2.2.2 Confidential Inferencing

An intuitive approach to apply confidential computing to the LLM service is serving multiple users with a single LLM instance running in a shared CVM (Figure 2b). This method is used by most existing commercial services, such as confidential inferencing in Azure [49] and AWS [47]. Although this approach effectively protects against malicious cloud providers and adversaries that compromise the cloud, it requires all users to fully trust the LLM provider and the CVM owner, which is not aligned with our threat model (§3.2).

An alternative approach is to instantiate a dedicated LLM instance for per-user CVM (Figure 2c). This setup offers stronger security, as each user is the owner of its associated CVM. However, this approach suffers from two significant

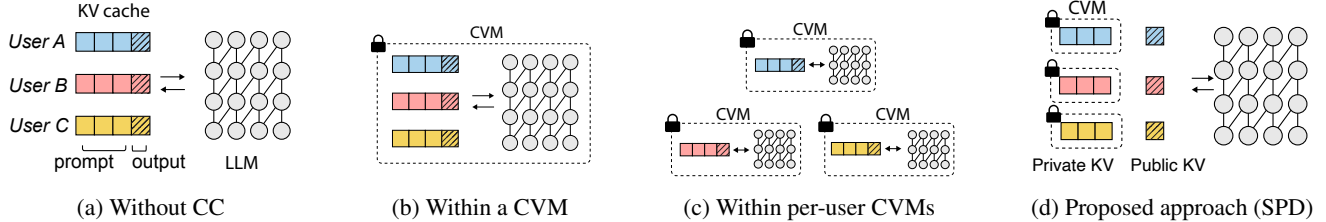


Figure 2: **Various LLM serving approaches.** (a) LLM serving without confidential computing (CC) is the most efficient, but user prompts are exposed to both the cloud infrastructure and the LLM provider. (b) Serving multiple users with a single CVM can protect against malicious cloud provider and adversaries on the cloud, but prompts remain exposed to the LLM provider. (c) Assigning a dedicated CVM per user offers higher level of protection, from both cloud infrastructure and LLM provider, but it is inefficient since each CVM contains its own copy of the LLM. (d) SPD strikes a balance between security and efficiency by isolating only the user’s prompt (and private KV cache) within the CVM, while allowing batch processing across users.

inefficiencies: (1) limited scalability, as the number of concurrent user CVMs is constrained, and (2) low throughput due to reduced batch parallelism. For example, a 13B-parameter LLM requires about 27 GB of memory for its weights using 16-bit floating point, which means that a 80 GB GPU can only support up to three concurrent user CVMs. Moreover, inference is performed independently for each user, e.g., X_1W, \dots, X_nW , which is less efficient than batching as $(X_1 : \dots : X_n)W$. Our solution, SPD, addresses both challenges by isolating only the user prompt within the CVM while sharing the LLM among multiple users (Figure 2d). However, we note SPD alone is less secure as it offloads majority of computation to out of CVMs, trading efficiency and scalability with minimal risk of secret leakage. Its goal is not to replace confidential inferencing solutions but to provide an alternative approach that fits different scenarios as discussed in §A.4.

Some prior work [51, 57, 61] aim to address the scalability problem by isolating multiple instances within a single CVM. These approaches either fail to use GPUs for acceleration, or do not provide the same security level as all instances must trust and share the software stack deployed within the CVM.

2.3 Chaffing and Winnowing

In an information-theoretic sense, a message is secure if an eavesdropper can do no better than guessing randomly to determine its content [33, 50]. Modern encryption achieves this by transforming messages into ciphertexts that are indistinguishable from random noise; in doing so, unfortunately, it renders the text meaningless to an LLM. In contrast, *chaffing and winnowing* [5, 48] secures message confidentiality without encrypting the message itself. In naïve chaffing and winnowing, a sender secures sensitive messages by mixing them with fake ones, known as *chaffing*. For example, to secure the message “Meet at 5pm”, the sender might transmit it along with variations like “Meet at Xpm”, where X ranges from 1 to 12. Assuming both the sender and the receiver share a symmetric secret key for signing and verifying a message

authentication code (MAC) sent along with a message, the receiver can authenticate whether a message originates from the sender. The sender includes a fake MAC with each fake message, which enables the receiver to identify and discard fake messages, known as *winnowing*.

2.4 Related Work

In recent years, researchers have explored various approaches beyond confidential computing to preserve the privacy of user prompts in LLM inference [14].

Differential Privacy protects prompt confidentiality by injecting noise into token distributions [42, 59], generating few-shot random examples [54], or tuning prompts [21]. However, these methods are task-specific and compromise output invariance. In contrast, SPD and PO maintain output invariance.

Multi-Party Computation (MPC)-based methods utilize *secret sharing* that cryptographically splits a number x , either an LLM weight or a prompt token, into multiple numbers, i.e., $x = x_1 \oplus x_2 \oplus \dots \oplus x_n$. Then they distribute each split x_i to an untrusted party. The user then derives the LLM inference output by cryptographically combing the outputs of these parties. This technique suffers from multiple problems. First, the compute parties must not collude. Second, secret sharing is not efficient for all LLM operations. Recognizing its inefficiency, the authors chose to modify the model, e.g., using ReLU instead of SoftMax [2], or use a much smaller model distilled specially [27], violating output invariance.

Homomorphic encryption (HE) enables computations on encrypted data and is often combined with MPC to guarantee end-to-end privacy in LLM inference [9, 19, 31, 43]. However, its significant overhead impedes its use in real-world applications, particularly for supporting nonlinear functions. Recent works [9, 31, 43] replace these functions with approximations, further impeding the use of existing well-trained models.

To our knowledge, other approaches [13, 29] do not protect the prompts from untrusted cloud hosted LLMs. For example, the *ensemble-only* method [13] mitigates the membership

inference attacks (MIAs) assuming the attackers have access only to the LLM’s prediction outputs. By the time of writing, OSPD is the first scalable design that applies confidential computing to LLM serving without trusting the LLM.

3 Design Overview

We introduce the design goals (§3.1) and threat model (§3.2) of Confidential Prompting, and an overview of OSPD (§3.3).

3.1 Design Goals

Our primary goal is to secure user prompt confidentiality in cloud-hosted LLM serving. Depending on whether the attackers have unlimited computational resources or not, we aim to protect the sensitive segments in user prompts, such as Personally Identifiable Information (PII), or the entire prompts. Beyond user prompt confidentiality, we target at another three goals in designing Confidential Prompting.

- **Model confidentiality:** Users must not know the weights of the cloud LLM. This is critical because the LLM’s weights constitute an intellectual property of the cloud LLM provider. Preserving model confidentiality enhances Confidential Prompting’s deployability in real-world.
- **Output invariance:** Protection measures must not change the output of the cloud LLM. We believe output invariance is crucial, particularly for tasks such as summarizing clinical notes, where even a small accuracy error could lead to serious consequences for users’ health.
- **Compute efficiency:** Protection measures must not significantly increase the cost. Though security is not free, we believe a more efficient approach is more attractive to users.

3.2 Trust and Threat

Trusted Computing Base (TCB) We assume the users’ local machines and the cloud’s computing hardware, such as CPUs and GPUs, are trustworthy. Particularly we trust the confidential computing related hardware’s architectural extensions, such as Intel TDX [23], AMD SEV [3] and Nvidia GPU CC [40]. This means that users can verify the integrity of their own Confidential Virtual Machines (CVMs) running in the cloud and once verified, these CVMs are trusted. Consequently, we treat a user and its CVM as the same party, even though the CVMs are hosted in the cloud.

We assume the communication channels between users and their CVMs are secure, for example, encrypted with TLS. However, as CVMs are hosted in the cloud, the cloud vendor can control the outbound network bandwidth allocated to CVMs, and inspect the outbound data. This bandwidth management and inspection are crucial to maintain model confidentiality while allowing the CVMs to read LLM weights.

Finally, we assume the users and their CVMs privately share the key (or seed) for a pseudorandom function (PRF).

Threat Model We consider the cloud vendor and the LLM provider as the same party, so called cloud LLM providers. We assume the users and the cloud LLM providers are mutually untrusted and seek to uncover other’s secrets. We adopt two variants of Honest-but-Curious (HBC) adversary model with respect to the cloud LLM providers. The only difference between the two variants is if the cloud LLM providers have (and are willing to use) unlimited computational resources to perform an attack. In these HBC variants, the cloud LLM providers faithfully follow the prescribed computation steps for LLM inference, but seek to extract user secrets in prompts.

We do not consider attacks that compromise the CVMs, the communication channels, or the pseudorandom function (PRF). Consequently, user prompts and the private KV cache remain securely within the CVMs, inaccessible to the cloud LLM provider (Figure 2d). However, under the HBC variant that the cloud LLM providers have unlimited computational resources, the providers may attempt reconstruction attacks to retrieve sensitive information stored in the CVMs.

Denial of service (DoS) attacks are out of scope in this work. We note that confidential computing systems generally assume stronger threat models than HBC. Confidential Prompting assumes a weaker threat model as it offloads most computations out of the CVMs for efficiency. We discuss possible strategies for a stronger threat model in §A.4.

3.3 OSPD Overview

Confidential Prompting aims to achieve all goals outlined in §3.1. As illustrated in Figure 1, its core design components, *Secure Partitioned Decoding (SPD)* and *Prompt Obfuscation (PO)*, collaborate to defend against the threat model in §3.2. We next provide a detailed overview of this collaboration.

Initialization To use OSPD for confidential prompting, a user creates its CVM on cloud in the same way as how a CVM is initialized in common cases. That is, the user first creates its CVM with a prototype of OSPD (§6) in the cloud, and verifies the CVM integrity through remote attestation. Next, the user encrypts its prompt locally before transmitting the prompt to the CVM, which can decrypt the prompt exclusively. During the entire setup, all communications are secure (§3.2).

Prompt Obfuscation (§5) PO has two steps to generate *virtual prompts*: (i) tagging sensitive segments in a prompt and (ii) sampling fake n-grams for each tagged segment.

For (i), a user can deploy any existing tools in its CVM to identify and tag sensitive segments in its prompt. The user can also train a small language model (SLM) for the tagging. For simplicity, we use Google’s PII detection tool to tag Personally Identifiable Information (PII) in our prototype (§6) as an example implementation.

For (ii), the CVM processes each tagged sensitive segment

S_{target} in the prompt S independently (§5.1). That is, the CVM samples a set of fake n-grams F , such that for each $S_{fake} \in F$,

$$\|P(S_{fake}|S - S_{target}) - P(S_{target}|S - S_{target})\| < \epsilon$$

where ϵ is an error bound parameter close to 0, and the operation $S_a - S_b$ returns the result of removing segment S_b from S_a . As for the probability function P , it returns the probability of a token sequence, modeled by a language model (LM).

The CVM generates λ *virtual prompts* with F and a random number idx with a pseudorandom function (PRF), serving as the index of the authentic prompt among $\lambda + 1$ prompts.

Prefill (§4.1) The CVM computes *private KV cache* for all $\lambda + 1$ prompts, always keeping these $\lambda + 1$ prompts and their private KV cache within the CVM without any exposure.

We note that the CVM requires LLM weights for the computation during prefill. Once the CVM gets the LLM weights from the cloud LLM providers, it is not allowed to send any data out of the cloud, except the output tokens in plaintext generated by the cloud LLM instance. The cloud vendor limits its network bandwidth and inspect all outbound data to avoid LLM weights leakage, thereby ensuring *model confidentiality*.

Secure Partitioned Decoding (§4.2) SPD partitions the attention score computation during decode phase into a two-party computation. That is, the CVM and the cloud LLM computes the private (A_{pvt}) and the public (A_{pub}) attention score respectively. Specifically, the private attention score A_{pvt} is computed with the private KV cache, which is already pre-computed during prefill and stored in the CVM. Consequently, the CVM does not require the LLM weights for computation during decode, thereby remaining a small footprint in decode and improving the scalability.

After computation, the CVM sends A_{pvt} to the cloud LLM, which then merges the A_{pvt} with the A_{pub} to get the full attention score. As the attention score decomposition is lossless, SPD allows the cloud LLM to generate tokens without compromising *output invariance*.

Additionally, SPD maintains *compute efficiency* as it allows the cloud LLM to batch process for multiple users, and the CVM memory footprint remains small during decode.

Complementarity between SPD and PO SPD and PO are complementary techniques that collaboratively defend against attacks which would likely succeed if either technique were employed independently. Firstly, SPD alone is vulnerable to reconstruction attacks. Conversely, like many existing obfuscation methods, an attacker can improve their chances of defeating PO by obtaining detailed knowledge of the distribution of virtual prompt generation through statistical analysis.

However, these attacks can breach OSPD only at a high cost and with a low probability of success. Within the OSPD framework, all $\lambda + 1$ prompts and their private KV cache securely reside within the CVM. The protection provided by SPD significantly increases the cost of collecting statistical information, such as performing reconstruction attacks

to extract all $\lambda + 1$ prompts and deduce distribution data. With limited statistical information under a certain amount of computational resources, an attacker gains little advantage in breaching PO beyond random guessing. Consequently, even in the worst-case scenario where an adversary reconstructs all $\lambda + 1$ prompts, the probability of accurately identifying the authentic prompt increases by merely ϵ compared to random guessing among the $\lambda + 1$ possible prompts.

Extract Authentic Response The CVM sends the responses of all $\lambda + 1$ prompts to the user. It is worth noting that the user already knows the index idx , as we assume the user and the CVM share the key of the PRF (§3.2). This allows the user to perform *winnowing* and extract the authentic response.

4 Efficient Prompt Protection with Confidential Computing

Keeping a dedicated copy of LLM weights in multiple CVMs leads to limited scalability as discussed in §2.2.2. This is the main obstacle to use per-user CVMs for LLM serving while untrusting the LLM provider. We solve this challenge by eliminating the need to store LLM weights in CVMs after the initial prefill phase. Our key insight is the decoding in LLMs can be formulated as a secure multi-party computation, where only one party needs access to the LLM weights. Specifically, we distinguish K, V attention states into *private* and *public* parts. The user prompt’s K, V states are private and are kept confidential in the CVM, while the generated tokens’ K, V states are public and shared with the LLM. For simplicity, we detail the protocol with one-user scenario as follows.

There are three participants in the protocol: (i) the user; (ii) the user’s CVM; and (iii) the cloud LLM.

1. **Prefill (§4.1):** The user sends a prompt to its CVM, which computes K_{Pvt}, V_{Pvt} states of the prompt and generates the first token. Then the CVM sends the token to the LLM.
2. **Decode (§4.2):** As in Figure 3, for each transformer layer:
 - (a) The cloud LLM computes $Q_{New}, K_{New}, V_{New}$ of the received token, appends K_{New}, V_{New} to K_{Pub}, V_{Pub} to maintain public KV cache, and sends Q_{New} to the CVM.
 - (b) The CVM responds with private attention score $A_{pvt} = \sigma(Q_{New} K_{Pvt}^T) V_{Pvt}$.
 - (c) The cloud LLM computes public attention score $A_{pub} = \sigma(Q_{New} K_{Pub}^T) V_{Pub}$, and merge A_{pvt} with A_{pub} to recover full attention score $Y = \sigma(Q_{New} K^T) V$ using Theorem 4.1.
 - (d) If it is the final layer, the output Y is sent to the CVM.
3. The CVM samples a new token from Y and sends it to the cloud LLM and the user. Then go to Step 2 until [EOS].

This protocol can be generalized to scenarios with multiple users, each with its own CVM operating in the cloud.

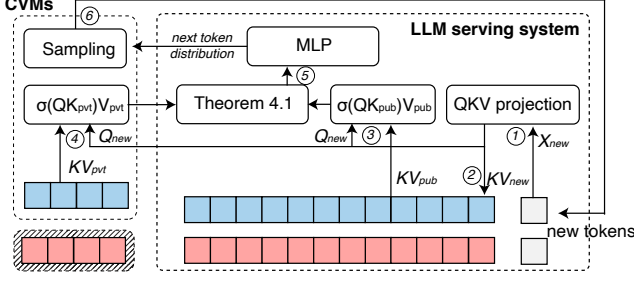


Figure 3: **SPD overview** on a simplified Transformer layer. The squares with various colors represent the KV cache associated with various users. ① Project hidden state X_{new} of a new token to $Q_{\text{new}}, K_{\text{new}}, V_{\text{new}}$. ② Append $K_{\text{new}}, V_{\text{new}}$ to the public KV cache. ③ Compute public attention (batch-process for all users). ④ Compute private attention in each user’s CVM. ⑤ Merge results for final attention output. The next token distributions are returned to user CVMs to sample and repeat the process.

4.1 Prefill in CVM

Upon receiving the n -token prompt from user, the CVM computes the attention states $K_{\text{Pvt}} \in \mathbb{R}^{n \times d}$ and $V_{\text{Pvt}} \in \mathbb{R}^{n \times d}$, and sends the first token to the cloud LLM. The LLM weights are discarded after prefill. We introduce an optimization to further reduce the CVM memory footprint: Since LLM weights are used only once, we employ a memory-efficient strategy where the CVM fetches the weights on demand and discards them after use, limiting memory usage to a single layer.

Security analysis of model confidentiality The CVM requires read-only access to the cloud LLM weights in the prefill phase. As mentioned in §3.2, the cloud vendor can inspect outbound data from the CVM, preventing LLM weights leakage to the user. The cloud LLM is able to check the integrity of the outbound data because it is the cloud LLM which generates the output tokens, knowing the exact value of the responses.

We note that even the use of PO (§5) does not require the CVM to send any encrypted data to the user during prefill and decode phases, otherwise forming a potential side channel to leak LLM weights. In particular, both the user and its CVM know the index of the authentic response among the $\lambda + 1$ candidates, without any communication after CVM initialization. This is because they share the key (or called seed) of the PRF and thus both already know the index in advance.

4.2 Secure Partitioned Decoding (SPD)

We formulate the decoding as a secure two-party computation based on the online softmax calculation [36], allowing the cloud LLM to retrieve the full attention score Y without knowing K_{Pvt} and V_{Pvt} . Specifically, we introduce the following theorem for two-party decoding:

Theorem 4.1 (Two-party attention computation). Let $K = \text{concat}(K_{\text{Pvt}}, K_{\text{Pub}}) \in \mathbb{R}^{n \times d}$, $V = \text{concat}(V_{\text{Pvt}}, V_{\text{Pub}}) \in \mathbb{R}^{n \times d}$, $Q \in \mathbb{R}^d$, and σ be a softmax function. Then,

$$\begin{aligned} \sigma(QK^\top)V &= \frac{\gamma_{\text{Pvt}}}{\gamma_{\text{Pvt}} + \gamma_{\text{Pub}}} \sigma(QK_{\text{Pvt}}^\top)V_{\text{Pvt}} \\ &+ \frac{\gamma_{\text{Pub}}}{\gamma_{\text{Pvt}} + \gamma_{\text{Pub}}} \sigma(QK_{\text{Pub}}^\top)V_{\text{Pub}} \end{aligned} \quad (1)$$

where $\gamma_{\text{Pvt}}, \gamma_{\text{Pub}}$ are denominators of each softmax operation, e.g. $\gamma_{\text{Pvt}} = \sum \exp(QK_{\text{Pvt}}^\top)$.

Theorem 4.1 is lossless and its proof is available in the appendix. This theorem serves as the foundation for the SPD design, which offers two key benefits. First, the cloud LLM can batch process all public states ($Q, K_{\text{Pub}}, V_{\text{Pub}}$) of different users in parallel using a single set of LLM weights. Second, computations in CVMs have a fixed cost and do not involve LLM weights, allowing the CVMs to retain only a small amount of memory for the private states. In addition, SPD only induces a constant communication overhead of $2d + 1$ floating points in each round. We note that computing γ_{Pvt} and γ_{Pub} individually is numerically unstable due to its exponential term. Instead, we compute $\gamma_{\text{Pvt}} = \sum \exp(QK_{\text{Pvt}}^\top - m_{\text{Pvt}})$, where $m_{\text{Pvt}} = \max(QK_{\text{Pvt}}^\top)$. The coefficients in Theorem 4.1 become $\frac{\gamma_{\text{Pvt}}}{\gamma_{\text{Pvt}} + \alpha\gamma_{\text{Pub}}}$ and $\frac{\gamma_{\text{Pub}}}{\alpha^{-1}\gamma_{\text{Pvt}} + \gamma_{\text{Pub}}}$, where $\alpha = \exp(m_{\text{Pub}} - m_{\text{Pvt}})$.

4.3 Security Analysis

User prompts and the private KV cache are confidential throughout their lifetime. Under the assumptions outlined in §3.2, user prompts are secured during transmission to the CVM. They remain in the CVM without any exposure in prefill phase. During decode, the CVM exposes only the private attention score A_{Pvt} , ensuring neither the prompt nor the private KV cache is directly exposed. The cloud LLM only has access to the generated tokens and the private attention score A_{Pvt} received from the CVM, which can not be directly reversed to uncover the prompt or the private KV cache.

This security analysis implies an attacker can uncover the private user prompt (or the embedding of the prompt $X_{\text{Pvt}} \in \mathbb{R}^{n_{\text{Pvt}} \times d}$, where $K_{\text{Pvt}} = X_{\text{Pvt}}W_K$ and $V_{\text{Pvt}} = X_{\text{Pvt}}W_V$) only via (semi) black-box reconstruction attacks. In a simpler case, the attacker can attempt to find an approximation of \tilde{X}_{Pvt} for

$$\|A_{\text{Pvt}} - \sigma(Q(\tilde{X}_{\text{Pvt}}W_K)^T)(\tilde{X}_{\text{Pvt}}W_V)\| = 0. \quad (2)$$

An attacker can also perform a stronger reconstruction attack using public KV cache of the generated tokens:

$$\begin{aligned} \|Y - \sigma(Q \times \text{concat}(\tilde{X}_{\text{Pvt}}W_K, K_{\text{Pub}})^T) \\ \times \text{concat}(\tilde{X}_{\text{Pvt}}W_V, V_{\text{Pub}})\| = 0 \end{aligned} \quad (3)$$

where Y is the result from Equation 1. It is worth noting that, an attempt to uncover a prompt directly from its known response is actually a reconstruction attack, which is usually

not as effective as Equation 3, because the latter contains more information, i.e., the distribution of the next token, than just the final output tokens.

Reconstruction attacks generally require a large number of observations to be effective. However, due to the autoregressive nature of LLMs, they can theoretically generate unlimited output tokens, resulting in a large number of public states.

To summarize, relying solely on SPD could secure the user prompt against typical adversaries who compromise the cloud but have limited computational resources. But it leaves the system vulnerable to adversaries who have unlimited computational resources to perform reconstruction attacks.

5 Prompt Obfuscation

We present *Prompt Obfuscation (PO)*, a novel defense against reconstruction attacks. Inspired by *chaffing and winnowing* [5, 48], PO aims to limit cloud LLM’s ability to accurately observe user prompts, at the cost of generating redundant tokens. The premise of chaffing and winnowing is that (1) an eavesdropper cannot distinguish between authentic and fake messages based on their content, while (2) the receiver can. PO achieves (1) by leveraging LLMs’ ability to perform infilling and (2) by exploiting the protocol’s reflective nature, in which the CVM sends intermediate data to the cloud LLM for processing and the output is reflected back to the CVM.

To obfuscate attackers and protect sensitive information in a user prompt, the CVM first identifies and tags sensitive segments in the prompt. Users can deploy any existing tools like Google’s PII detection or train a small language model (SLM) for tagging automatically. Then the CVM generates λ virtual prompts by replacing the sensitive segments with sampled fake n-grams. Figure 14 in §A.3 is an example. These λ virtual prompts and their private KV cache always reside in the CVM, in the same way as the authentic one. The CVM and the cloud LLM collaborate to decode all $\lambda + 1$ prompts in parallel, with the cloud LLM being unable to distinguish the virtual prompts from the authentic one. Only the user and its CVM know which prompt and response are authentic.

5.1 Sampling Virtual Prompts

We introduce Greedy Quantized Sampling (GQS), a simple algorithm designed to sample fake n-grams based on the user’s prompt S , as illustrated in Algorithm 1. We assume the automatic tagging tool marks sensitive segments, i.e., sensitive token subsequences, with `<redacted/>` tags. For simplicity, we assume the sensitive subsequences within a prompt are independent and the CVM processes them one by one, denoted S_{target} . The target subsequence S_{target} may represent a name, location, medical condition, or other sensitive information. The goal of GQS is to generate multiple fake replacement subsequences that appear as authentic as the original S_{target} . In addition to S and S_{target} , GQS requires parameters ϵ and

λ_{max} , as well as a pre-trained language model LM . For brevity, we denote the algorithm as $GQS(S, S_{target}, \epsilon)$.

Algorithm 1 leverages the ability of LLMs to infill missing subsequence in a prompt, that is, replacing S_{target} with $S_{fake} \in F$. Some LLMs are trained for infilling tasks [4, 11, 12]. It has also been shown that simple autoregressive LLMs can perform infilling when the prompts are appropriately formatted [39], such as using the *Format* function to obtain the formatted prompt \tilde{S} in Algorithm 1. Sequences $\{Ctrl_i\}$ refer to predefined control sequences used to format the prompt, which are determined by the chosen language model LM . For example, tokens like `<prefix>` and `<suffix>` are commonly used in fill-in-the-middle (FIM) models [28].

There are two key parameters in GQS that control the number of fake n-grams to generate: $0 < \epsilon \leq 1$ and $\lambda_{max} \in \mathbb{N}$. ϵ is the error bound for the fake n-grams, while λ_{max} controls the maximum number of candidates to consider at each step. These parameters adjustable according to security requirements and the CVM’s available memory. Given the prompt S and the target subsequence S_{target} , the CVM samples a set of fake n-grams F using $GQS(S, S_{target}, \epsilon)$ and constructs a set of virtual prompts by replacing S_{target} with $S_{fake} \in F$. The user may provide an additional parameter, λ_{min} . If fewer than λ_{min} virtual prompts are generated, the CVM will stop and alert the user to a potential information leak if it continues.

In the case where multiple sensitive subsequences are marked with `<redacted/>` tags in a prompt, since conditioning the fake n-grams on all subsequences simultaneously is impractical due to the exponential growth in the number of candidates, we treat each selected subsequence as an independent variable. Fake n-grams are sampled for each subsequence in parallel using GQS. Under the assumption of independence, the upper bound of ϵ of the generated virtual prompts is equal to the sum of the values ϵ_i for each i -th subsequence.

Compact Representation of Virtual Prompts We introduce a memory-efficient approach to store virtual prompts within CVMs. This approach significantly reduces memory overhead while introducing a small approximation error to the decoding of virtual prompts. It does not affect the final accuracy, as the decoding of the authentic prompt remains unaffected, and the virtual ones are eventually discarded.

Given λ virtual prompts, instead of storing all K_{Pvt} and V_{Pvt} for each virtual prompt, which would require memory proportional to $\lambda|S|$, we compute the attention states for the shared part $S - S_{target}$ separately, and share them across all virtual prompts, but not for the authentic prompt. This allows the CVM to store attention states only for the individual fake n-grams $S_{fake} \in F$, reducing the memory cost to store all virtual prompts from $\lambda|S|$ to $|S - S_{target}| + \lambda|S_{target}|$.

5.2 Security Analysis

In §3.3, we analyze SPD and PO are complementary and collaboratively defend against attacks that would likely suc-

Algorithm 1 Greedy Quantized Sampling (GQS) for Prompt Obfuscation

Require: User’s prompt S as token sequence, target subsequence S_{target} , parameters ϵ and λ_{max} . LM is a pre-trained language model, and $\{Ctr_i\}$ are the associated pre-defined control sequences to format the prompt. The $+$ operator indicates concatenation, while $S_a - S_b$ indicates removing subsequence S_b from S_a .

- 1: $S_{\text{context}} \leftarrow S - S_{\text{target}}$
- 2: $n \leftarrow |S_{\text{target}}|$
- 3: $\tilde{S} \leftarrow \text{Format}(\{Ctr_i\}, S_{\text{context}}, n)$ ▷ Format \tilde{S} for the infilling task.
- 4: $\epsilon' \leftarrow \epsilon/n$
- 5: $F \leftarrow \{\{\}\}$
- 6: **for** $i \leftarrow 1$ to n **do**
- 7: $F_{\text{new}} \leftarrow \{\}$
- 8: $X_{\text{ref}} \sim LM(\tilde{S} + S_{\text{target}}^{1\dots i-1})$ ▷ LM models the distribution of the next token.
- 9: $\rho \leftarrow P(X_{\text{ref}} = S_{\text{target}}^i)$ ▷ Compute the reference probability ρ
- 10: **for each** $S_{\text{fake}} \in F$ **do** ▷ Find all tokens with probability within the same quantized bin as ρ .
- 11: $X \sim LM(\tilde{S} + S_{\text{fake}})$ ▷ Each “bin” has a width of ϵ' . There are $\lceil \frac{1}{\epsilon'} \rceil$ bins in total.
- 12: $F_{\text{new}} \leftarrow F_{\text{new}} \cup \{S_{\text{fake}} + x \mid \lfloor \frac{\rho}{\epsilon'} \rfloor \cdot \epsilon' < P(X = x) \leq (\lfloor \frac{\rho}{\epsilon'} \rfloor + 1) \cdot \epsilon'\}$
- 13: **end for**
- 14: $F \leftarrow \text{top-}\lambda_{\text{max}}(F_{\text{new}})$ ▷ Only select λ_{max} candidates to keep the compute cost static.
- 15: **end for**
- 16: **return** F

ceed if either technique were employed independently. In this section, we analyze in the worst case where an attacker reconstructs all $\lambda + 1$ prompts, the probability of correctly guessing the authentic prompt is $\epsilon + 1/(\lambda + 1)$, assuming the language model LM accurately captures the true distribution \mathcal{D} .

Security Model The key of analyzing PO is how to *quantify* “*authenticity*” of virtual prompts. To achieve this, we introduce the concept of ϵ -close over a distribution \mathcal{D} to bound the “distance” between two sets of messages:

Definition 5.1 (ϵ -close over \mathcal{D}). Two sets of messages S and S' are ϵ -close over \mathcal{D} if $\max_{s \in S, s' \in S'} |P_{\mathcal{D}}(s) - P_{\mathcal{D}}(s')| < \epsilon$, where $P_{\mathcal{D}}(s)$ represents the probability of a message s as modeled by the distribution \mathcal{D} .

\mathcal{D} refers to the true language distribution, which may not be known to the user or any party. The language model LM used by the user to create the fake n-grams can approximate \mathcal{D} , denoted as \mathcal{D}_{LM} . We define the “distance” between two distributions over a set of messages U as

$$\Delta_U(\mathcal{D}, \mathcal{D}_{LM}) = \max_{s \in U} |P_{\mathcal{D}}(s) - P_{\mathcal{D}_{LM}}(s)|.$$

If $\Delta_U(\mathcal{D}, \mathcal{D}_{LM})$ is close to zero, we say LM provides a sufficiently accurate approximation of \mathcal{D} over subdomain U .

Intuitively, if there are λ virtual prompts that are ϵ -close to the authentic one over \mathcal{D} and ϵ is small, these virtual prompts appear authentic, as their probabilities are close to that of the authentic one, bounded by ϵ . In the case that ϵ closes to zero, $P_{\mathcal{D}}(s)$ is about the same for all s from these prompts. In other words, even if an adversary knows \mathcal{D} and obtains the plaintext of all $\lambda + 1$ prompts, it can only guess randomly, with a probability of approximately $\frac{1}{\lambda+1}$ of being correct, and an advantage bounded by ϵ .

Worse Case Analysis [Theorem 5.2](#) implies that if both ϵ and Δ are small, the virtual prompts generated as described in [§5.1](#) would appear as authentic as the user prompt S .

Theorem 5.2. *Given a user prompt S and a subsequence S_{target} , let $F = GQS(S, S_{\text{target}}, \epsilon)$ and $\Delta = \Delta_U(\mathcal{D}, \mathcal{D}_{LM})$, where $U = \{S_{\text{target}}\} \cup F$. Then $\{S_{\text{target}}\}$ and F are $(\epsilon + 2\Delta)$ -close over \mathcal{D} .*

More precisely, the maximum difference between the probabilities of any pair of authentic and fake subsequences is $\epsilon + 2\Delta$, given S as context. The proof is provided in the appendix. Suppose that we have an authentic prompt S and a set of virtual prompts $S_1, S_2, \dots, S_{\lambda}$. Let \mathcal{D}_{LM} be the distribution of all possible sequences modeled by LM . [Theorem 5.2](#) essentially states that an adversary with knowledge of \mathcal{D} can guess the authentic prompt S with a probability $\epsilon + 2\Delta$ better than randomly choosing from $\lambda + 1$ possible prompts. Therefore, the security of PO can be characterized by three factors: (1) the set size, λ ; (2) the error bound of sampling, ϵ ; and (3) the gap between the true distribution and its approximation, $\Delta = \Delta_U(\mathcal{D}, \mathcal{D}_{LM})$.

In some cases, \mathcal{D} can be well captured by \mathcal{D}_{LM} . A clear example is when the number of alternative prompts is finite and enumerable, such as “I live in [CITY]” and “I am [AGE] years old”. In such cases, PO satisfies the definition of confidentiality with a reasonably small ϵ and a large λ . Empirical evaluation results are provided in [§7.1](#).

However, PO does not fully guarantee confidentiality when the true distribution \mathcal{D} differs from \mathcal{D}_{LM} . This can happen when \mathcal{D}_{LM} is simply not sufficiently sophisticated. In such cases, PO serves as an *obfuscation*, as its name suggests, increases the cost of cryptanalysis, but does not fully prevent it. The above analysis suggests that an adversary with greater

knowledge of the true distribution \mathcal{D} gains an advantage in guessing. However, it is important to note that \mathcal{D} is not always accessible to adversaries, meaning the actual error bound in practice is likely smaller than our theoretical analysis.

Another scenario in which PO does not provide full confidentiality is when the prompt S is unique. In such cases, it may be impossible to generate fake n-grams without using a large ϵ or small λ , regardless of whether \mathcal{D} is well captured by \mathcal{D}_{LM} or not. To prevent a potential information leak, PO allows users to configure the desired ϵ and λ_{min} . If $\lambda < \lambda_{\text{min}}$, the CVM will stop in the prefill phase and alert the user.

Finally, the security of PO also depends on whether an adversary can successfully guess the index of the authentic prompt among $\lambda + 1$ prompts, even without reconstructing all prompts. PO employs a pseudorandom function (PRF) to generate the index. As stated in §3.2, attacks on the PRF are outside the scope of our threat model.

6 Implementation

We implement OSPD (SPD+PO) based on PyTorch and target the widely adopted Llama [55] series of open-source LLMs. We next describe a few key implementations in our prototype.

LLM Serving Server. We develop an LLM serving server based on the Transformers library [58], which assumes all user requests arrive simultaneously (no continuous batching) for simplicity. To support SPD, we adapted the Llama model by monkey-patching its attention module. We modified the attention score calculation to asynchronously send the query tensor (Q in Theorem 4.1) to each user via the GLOO tensor communication backend [16]. This allows us to receive private attention scores from users while computing public attention scores in parallel. The server waits for all private scores to arrive before evaluating the final attention score.

Prompt Vault. Within each user’s CVM, a client called the prompt vault manages operations like prefill, PO, and calculating private attention scores. The prompt vault synchronously listens to the LLM serving server to receive the Q tensor over the GLOO backend and returns results based on Theorem 4.1.

Serving virtual prompts with sub-linear memory. We implement the compact representation mechanism for virtual prompts (§5.1) using asymmetric attention masks. For example, suppose we have two prompts—real and fake—sharing a common segment S_{shared} of length a . The real sequence’s KV cache is S_{real} , and the fake one is S_{fake} , both of length b . The naive way to store attention states is to batch them:

$$(K \quad V) = \begin{pmatrix} S_{\text{shared}} & S_{\text{real}} \\ S_{\text{shared}} & S_{\text{fake}} \end{pmatrix} \in \mathbb{R}^{2 \times 2(a+b) \times d}. \quad (4)$$

Instead, our implementation flattens the attention states to eliminate redundancies:

$$(K \parallel V) = (S_{\text{shared}} \quad S_{\text{real}} \quad S_{\text{fake}}) \in \mathbb{R}^{1 \times (a+2b) \times d}. \quad (5)$$

We use a special attention mask where 1_n and 0_n denote vectors of ones or zeros of size n :

$$M = \begin{pmatrix} 1_{\text{shared}} & 1_{\text{real}} & 0_{\text{fake}} \\ 1_{\text{shared}} & 0_{\text{real}} & 1_{\text{fake}} \end{pmatrix} \in \{0, 1\}^{2 \times (a+2b)}. \quad (6)$$

The attention formula in § 2.1 then becomes:

$$Y = \text{softmax} \left(\frac{QK^T}{\sqrt{d}} \right) M^T V \in \mathbb{R}^d. \quad (7)$$

Note that approaches like pagedattention [25] can be considered for achieving the same effect, but they are not yet fully compatible with CVMs.

7 Evaluation

Our evaluation primarily aims to address two questions:

- Does OSPD preserve prompt confidentiality in practice?
- Does OSPD maintain compute efficiency, considering model confidentiality and output invariance are intuitive?

To answer the first question, we empirically examine the maximum available λ for the desired error bounds given by ϵ , which are referred to as pairs of security factors (ϵ, λ) in the following, and examine other factors that influence the sampling results. Subsequently, we evaluate the performance of OSPD compared to two naive CVM methods (Figure 2).

Evaluation setup. Our evaluation utilizes the Llama 2 [55] models with 7B and 13B parameters, Llama 3 [35] model with 8B parameters, and Code Llama [34] model with 34B parameters. All experiments were conducted on a cloud node equipped with an NVIDIA H100 NVL GPU with 94 GB of memory, 40 AMD EPYC Genoa processor cores, and 320 GB of system memory. Architectural security features such as AMD SEV-SNP [3] and NVIDIA GPU CC [40] are enabled for evaluation that require confidential computing. We note that our design does not require confidential computing protection for the LLM serving server. However, since computing nodes with multiple GPUs that support enabling GPU CC feature were not available at the time of writing, and because NVIDIA GPU CC feature can only be enabled or disabled entirely on a single GPU, the confidential computing overhead also applies to the LLM server in the following experiments. Consequently, the performance overhead presented in this section is higher than the ideal case described in our design.

7.1 Security of Prompt Obfuscation

As discussed in §5.2, the security of Prompt Obfuscation depends on the pair of security factors (ϵ, λ) and the distance $\Delta_U(\mathcal{D}, \mathcal{D}_{\text{LM}})$. Here, \mathcal{D} represents the *true distribution* of prompts, which is inaccessible to both users and adversaries. We assume that \mathcal{D}_{LM} provides a sufficiently accurate approximation of \mathcal{D} . Based on this assumption, we empirically examine the pairs of security factors (ϵ, λ) in different categories of personally identifiable information (PII).

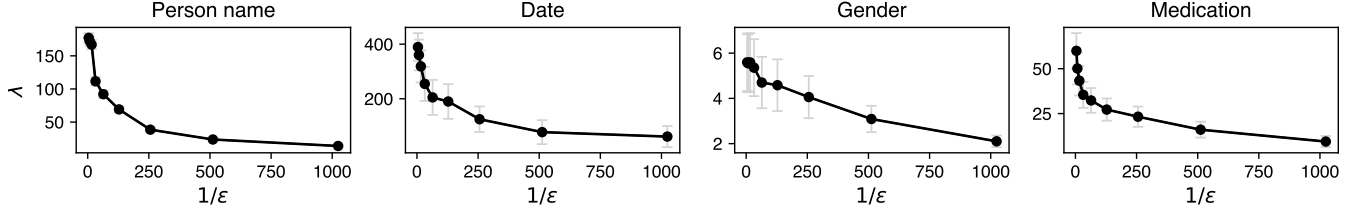


Figure 4: (ϵ, λ) pairs sampled from the clinical dataset with $\lambda_{\max} = 512$, for four selected PII categories (person name, date, gender and medication). Dots indicate the mean of λ for each ϵ , and the error bars indicate a 95% interval.

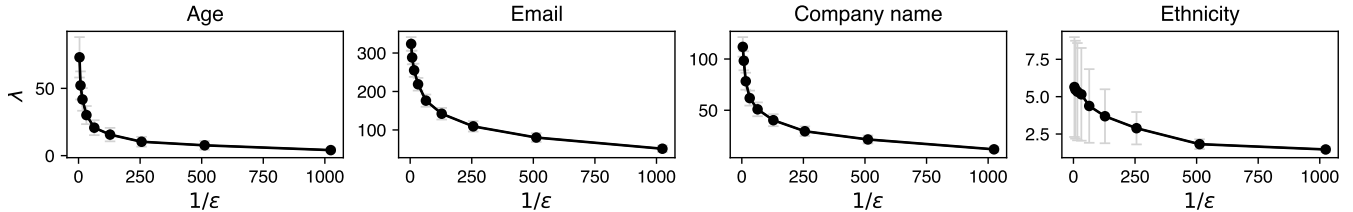


Figure 5: (ϵ, λ) pairs sampled from the resume dataset with $\lambda_{\max} = 512$, for four selected PII categories (age, email, company name and ethnicity). Dots indicate the mean of λ for each ϵ , and the error bars indicate a 95% interval.

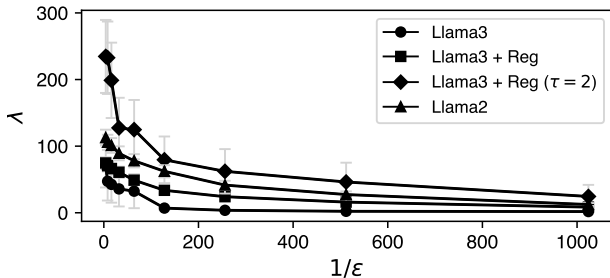


Figure 6: (ϵ, λ) pairs sampled from the clinical dataset with $\lambda_{\max} = 512$, for locational PII, e.g. name of places. Unless otherwise specified, the sampling temperature is set to $\tau = 1$.

Dataset Preparation. We first construct the clinical dataset by combining clinical dialogues between patients and physicians [6] with clinical notes from USMLE Step 2 [38]. Additionally, we use a public resume classification dataset from Kaggle [37]. To categorize and tag the PII data, we use Google’s PII detection tool, marking each instance with a tag `<redacted/>`. Details are provided in the appendix.

Exhaustive Sampling. We present the results for the examined pairs of security factors (ϵ, λ) in different categories of PII in Figure 4 and Figure 5. These value pairs are determined through an exhaustive search using the GQS algorithm (Algorithm 1) on both datasets, with Llama 3 model, $\lambda_{\max} = 512$, and the sampling temperature $\tau = 0$.

Result Analysis. Our observations indicate that GQS can generate a reasonably large set of fake n-grams. For example, with $\epsilon = 0.1$, the “date” category has approximately $\lambda = 320$, which roughly corresponds to the number of days in a year, and the “age” category has $\lambda = 52$, reflecting age groups from 20 to 70. Examples of dataset samples and GQS outputs are

provided in the appendix.

Effect of Different Models and Parameter Size. The impact of the model parameter size on λ is relatively small. For example, comparing Llama 2 models with 7B and 13B parameters on the clinical dataset results in only a 4% difference in λ . In contrast, the choice of language model has a more substantial effect on λ . In Figure 6, there is a $2.4\times$ difference in λ between Llama 3 and Llama 2 (13B). We observed that Llama 3, as a more advanced model than Llama 2, is more “confident” in selecting the next token, which narrows the possible candidate pool. In other words, the distribution modeled by Llama 2 is flatter, resulting in a higher λ under the same conditions.

Effect of Regularization. Grammar and typing errors in the target sequence S_{target} degrade the security of prompt obfuscation, as sequences with such errors are far less common in the distribution. Regularizing the content, such as correcting capitalization and spelling, can improve λ . We use a ChatGPT-based tool to correct typing errors in the dataset and compare the λ in Figure 6 between regularized (“Llama3+Reg”) and non-regularized (“Llama3”) datasets.

Effect of Sampling Temperature. The λ values are influenced by the token sampling temperature τ . A higher τ flattens the token distribution, increasing the number of fake n-grams that fall within the same ϵ' bin as the authentic n-gram (Algorithm 1). We present the difference in λ between $\tau = 1$ (“Llama3+Reg”) and $\tau = 2$ in Figure 6, indicating that prompt obfuscation can be more effective with a higher setting τ .

7.2 Performance Analysis

We implement two baselines for performance evaluation to demonstrate the scalability and compute efficiency of our approach: (1) *No protection*, a naive approach where every user

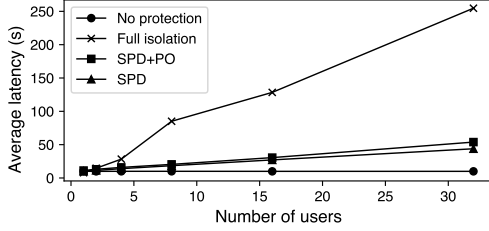


Figure 7: **Average latency with varying number of users**, served with Llama 2 (13B), 64 input tokens, 64 output tokens, and $\lambda = 8$ for the benchmark with PO.

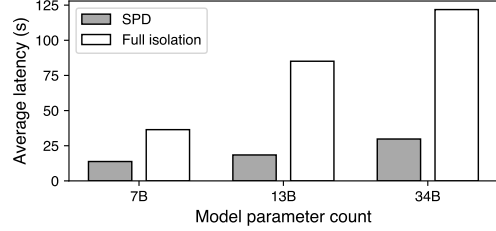


Figure 8: **Average latency with different model sizes**, measured by parameter count, with 8 users, 64 input tokens and 64 output tokens.

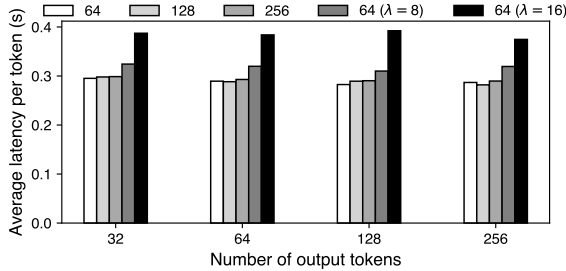


Figure 9: **Average latency in generating per output token, with varying number of input, output tokens and λ** , served with Llama 2 (13B) and for 8 users. Different groups of bars indicate different number of output tokens. The first three bars in each group indicate different input token counts while $\lambda = 0$. The other two bars in each group indicate different λ with 64 input tokens.

is served with a LLM instance within a CVM (Figure 2b), which is intended to demonstrate the upper bound for the performance with confidential computing; and (2) *Full isolation*, a naive approach where each user is served with a dedicated LLM instance in a per-user CVM (Figure 2c). Our approach is denoted as *SPD* (Figure 2d). We compare the performance of our approach with that of *Full isolation* because the latter defends against a similar threat model as ours.

7.2.1 Scalability

Our evaluation setup includes 1 to 32 users, with prompts ranging from 64 to 256 input tokens and generating between 32 to 256 output tokens per user. We measure the average end-to-end latency for each user to receive the output tokens. Figure 7, Figure 8 and Figure 9 summarize the main results, demonstrating that our approach scales more effectively than the *Full isolation* baseline as the number of users, input/output tokens, and the model parameter size increase.

Number of Users. The primary challenge in using CVMs for LLM services is achieving scalability with a growing number of users (§2.2). *Full isolation* handle separate instances of the LLM for each user, which limits the maximum number

of concurrent user CVMs due to GPU memory limitations. As shown in Figure 7, the latency of *Full isolation* increases significantly as the number of users increases. In contrast, the *SPD* approach scales effectively with the number of users, because it can host a large number of user CVMs concurrently.

Model Parameter Size. The *Full isolation* baseline also faces scalability challenges as model parameter sizes increase. In contrast, *SPD* is less affected by parameter size scaling. As presented in Figure 8, *Full isolation*'s end-to-end latency scales at a higher rate than that of *SPD* under the same conditions, when the model size increases from 7B to 34B.

Number of Input/Output Tokens. The number of input tokens primarily impacts the initial time-to-first-token (TTFT) latency. Both *Full isolation* and *SPD* experience a $15\times$ higher TTFT latency compared to the *No protection* baseline due to the absence of batch parallelism during the prefill phase. In contrast, the number of input tokens has negligible impact on the end-to-end latency in *SPD*, which reflects the time of decoding. As shown in Figure 9, the three bars in each group represent end-to-end latency for different input token counts such as 64, 128 and 256, with negligible differences among them, across different combinations of output token count and λ . Meanwhile, the increase of output token count also has negligible impact on latency per token, as decoding each token has static overhead.

7.2.2 Compute efficiency

We further analyze the overhead of OSPD along with its breakdown, to demonstrate our design is computationally efficient.

Overhead of Secure Partitioned Decoding. Secure Partitioned Decoding introduces overhead due to (1) confidential computation (CC), (2) the absence of batch processing in CVMs, and (3) communication between CVMs and the LLM. For (1), Figure 10 illustrates the impact of confidential computing (CC) on the *No protection* baseline and *SPD*. It shows that CC results in approximately 15% overhead compared to traditional computing without CC. For (2) and (3), we present SPD's latency breakdown in Figure 11. The six latency sources align with the processing steps in Figure 3. The QKV projection, public attention computation and MLP are

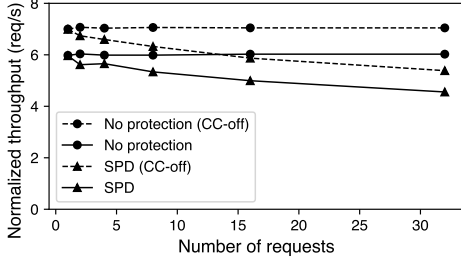


Figure 10: **Normalized throughput** with varying number of requests, 13B model, 64 input and 64 output tokens. “CC-off” indicates the throughput of conducting the benchmarks under the same condition with CC features disabled.

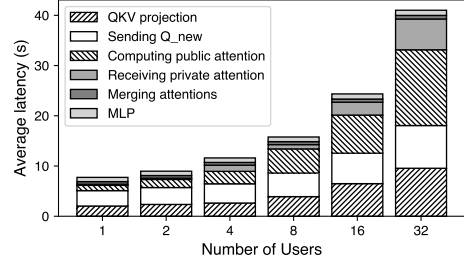


Figure 11: **Overhead breakdown of SPD** in the 13B model. As the number of users increases, the communication overhead of sending Q and receiving private attention increases linearly.

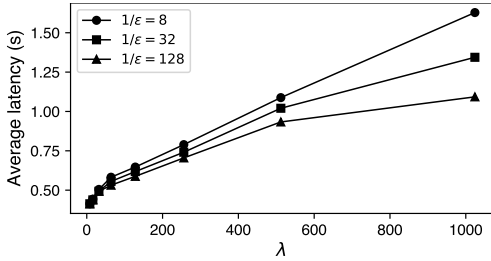


Figure 12: Average latency of sampling virtual prompts with varying λ_{\max} and ϵ for eight-token replacement in Llama 3.

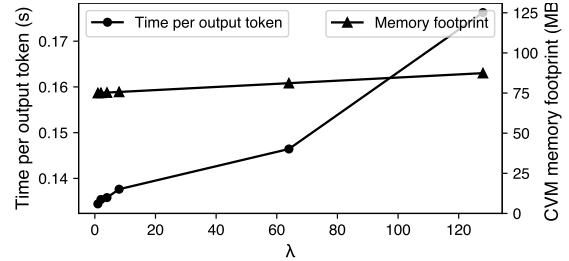


Figure 13: Average latency in generating per output token, and CVM memory footprint, with varying λ , for one user.

common in traditional decoding. However, the unique overhead introduced by SPD stems from the other three sources. Notably, the “Receiving private attention” latency includes both the time the cloud LLM spends waiting for private attention computation to finish and the communication cost. This encapsulates the overhead from (2) and (3), as either the absence of batch processing or high communication costs can cause the LLM to remain idle. As shown in Figure 11, the latency of (2) and (3) (“Sending Q_{new} ” and “Receiving private attention”) dominates the overhead, accounting for up to 40% of the total latency. In contrast, the overhead from merging attentions is relatively minor.

Overhead of Prompt Obfuscation. Prompt Obfuscation introduces overhead due to (1) sampling fake n-grams for virtual prompts, which increases TTFT, and (2) decoding for λ virtual prompts. For (1), Figure 12 illustrates the sampling latency for virtual prompts. The average sampling time for an eight-token replacement using $\lambda = 512$ and $\epsilon = 1/32$ is around 1 second. Sampling multiple subsequences can be batched, for example, 16 subsequences take about 1.5 seconds. Lower ϵ results in faster sampling due to a reduced λ . For (2), the impact of decoding virtual prompts on latency is shown in Figure 13. When $\lambda \leq 8$, the overhead is less than 3%. However, the overhead increases as λ grows: at $\lambda = 64$ and $\lambda = 128$, the overhead is approximately 7% and 30%, respectively. This overhead also scales with the number of users. As shown in Figure 9, for 8 users, the overhead of $\lambda = 8$ and $\lambda = 16$ is

around 8% and 25%, respectively. Fundamentally, the overhead grows with the total number of prompts increases, as the LLM processes user prompts and virtual prompts equally. On the other hand, virtual prompts impose minimal overhead on the CVM memory footprint, thanks to our memory-efficient approach for storing virtual prompts (§5.1). In summary, the use of PO and its associated overhead reflects a key trade-off in our design, as outlined in §3.1, that is balancing prompt confidentiality (§5.2) with compute efficiency.

8 Concluding Remarks

Cloud-based LLM services are becoming pervasive in our daily lives, but raise privacy concerns since users must submit their prompts to the cloud. OSPD combines two techniques to protect user prompts from LLM providers: secure partitioned decoding (SPD) and prompt obfuscation (PO). SPD fully leverages the confidential computing capabilities of modern hardware for efficient and scalable confidential prompting. PO, on the other hand, leverages the statistical properties of the LLM itself to achieve confidentiality without encryption. Our proposed techniques have the potential to enable privacy-preserving LLM applications such as chatbots and AI assistants that interact with a large number of end users, without high operational costs.

References

- [1] Josh Achiam, Steven Adler, Sandhini Agarwal, Lama Ahmad, Ilge Akkaya, Florencia Leoni Aleman, Diogo Almeida, Janko Altenschmidt, Sam Altman, Shyamal Anadkat, et al. Gpt-4 technical report. *arXiv preprint arXiv:2303.08774*, 2023.
- [2] Yoshimasa Akimoto, Kazuto Fukuchi, Youhei Akimoto, and Jun Sakuma. Privformer: Privacy-preserving transformer with mpc. In *2023 IEEE 8th European Symposium on Security and Privacy (EuroS&P)*, pages 392–410. IEEE, 2023.
- [3] AMD. AMD secure encrypted virtualization (SEV). <https://www.amd.com/en/developer/sev.html>, 2023.
- [4] Mohammad Bavarian, Heewoo Jun, Nikolas Tezak, John Schulman, Christine McLeavey, Jerry Tworek, and Mark Chen. Efficient training of language models to fill in the middle. *arXiv preprint arXiv:2207.14255*, 2022.
- [5] Mihir Bellare and Alexandra Boldyreva. The security of chaffing and winnowing. In *Advances in Cryptology—ASIACRYPT 2000: 6th International Conference on the Theory and Application of Cryptology and Information Security Kyoto, Japan, December 3–7, 2000 Proceedings 6*, pages 517–530. Springer, 2000.
- [6] Asma Ben Abacha, Wen-wai Yim, Yadan Fan, and Thomas Lin. An empirical study of clinical note generation from doctor-patient encounters. In *Proceedings of the 17th Conference of the European Chapter of the Association for Computational Linguistics*, pages 2291–2302, Dubrovnik, Croatia, May 2023. Association for Computational Linguistics.
- [7] Tom Brown, Benjamin Mann, Nick Ryder, Melanie Subbiah, Jared D Kaplan, Prafulla Dhariwal, Arvind Neelakantan, Pranav Shyam, Girish Sastry, Amanda Askell, et al. Language models are few-shot learners. *Advances in neural information processing systems*, 33:1877–1901, 2020.
- [8] Confidential Computing Consortium (CCC). The Linux Foundation Projects. <https://confidentialcomputing.io/>, 2023.
- [9] Tianyu Chen, Hangbo Bao, Shaohan Huang, Li Dong, Binxiang Jiao, Daxin Jiang, Haoyi Zhou, Jianxin Li, and Furu Wei. The-x: Privacy-preserving transformer inference with homomorphic encryption. *arXiv preprint arXiv:2206.00216*, 2022.
- [10] Yu Chen, Tingxin Li, Huiming Liu, and Yang Yu. Hide and seek (has): A lightweight framework for prompt privacy protection. *arXiv preprint arXiv:2309.03057*, 2023.
- [11] Jacob Devlin, Ming-Wei Chang, Kenton Lee, and Kristina Toutanova. Bert: Pre-training of deep bidirectional transformers for language understanding. *arXiv preprint arXiv:1810.04805*, 2018.
- [12] Chris Donahue, Mina Lee, and Percy Liang. Enabling language models to fill in the blanks. *arXiv preprint arXiv:2005.05339*, 2020.
- [13] Haonan Duan, Adam Dziedzic, Mohammad Yaghini, Nicolas Papernot, and Franziska Boenisch. On the privacy risk of in-context learning. *arXiv preprint arXiv:2411.10512*, 2024.
- [14] Kennedy Edemacu and Xintao Wu. Privacy preserving prompt engineering: A survey. *arXiv preprint arXiv:2404.06001*, 2024.
- [15] EU. General Data Protection Regulation (GDPR). <https://gdpr-info.eu/>, 2016.
- [16] Facebook. Gloop: Collective Communications Library, 2023. Accessed: 2024-11-09.
- [17] Paul Farrell. JPMorgan restricts ChatGPT usage for its 250K staff over fears it could steal sensitive banking secrets. <https://www.dailymail.co.uk/news/article-11780501/JPMorgan-restricts-ChatGPT-usage-250-000-staff-data-privacy-fears.html>, 2023.
- [18] In Gim, Guojun Chen, Seung-seob Lee, Nikhil Sarda, Anurag Khandelwal, and Lin Zhong. Prompt cache: Modular attention reuse for low-latency inference. *arXiv preprint arXiv:2311.04934*, 2023.
- [19] Meng Hao, Hongwei Li, Hanxiao Chen, Pengzhi Xing, Guowen Xu, and Tianwei Zhang. Iron: Private inference on transformers. *Advances in neural information processing systems*, 35:15718–15731, 2022.
- [20] US HHS. Health Insurance Portability and Accountability Act of 1996 (HIPAA). <https://www.cdc.gov/php/php/resources/health-insurance-portability-and-accountability-act-of-1996-hipaa.html>, 1996.
- [21] Junyuan Hong, Jiachen T Wang, Chenhui Zhang, Zhangheng Li, Bo Li, and Zhangyang Wang. Dp-opt: Make large language model your privacy-preserving prompt engineer. *arXiv preprint arXiv:2312.03724*, 2023.
- [22] Zhicong Huang, Wen-jie Lu, Cheng Hong, and Jian-sheng Ding. Cheetah: Lean and fast secure two-party

- deep neural network inference. In *31st USENIX Security Symposium (USENIX Security 22)*, pages 809–826, 2022.
- [23] Intel. Intel trust domain extensions (Intel TDX). <https://www.intel.com/content/www/us/en/developer/articles/technical/intel-trust-domain-extensions.html>, 2023.
- [24] Zhigang Kan, Linbo Qiao, Hao Yu, Liwen Peng, Yifu Gao, and Dongsheng Li. Protecting user privacy in remote conversational systems: A privacy-preserving framework based on text sanitization. *arXiv preprint arXiv:2306.08223*, 2023.
- [25] Woosuk Kwon, Zhuohan Li, Siyuan Zhuang, Ying Sheng, Lianmin Zheng, Cody Hao Yu, Joseph Gonzalez, Hao Zhang, and Ion Stoica. Efficient memory management for large language model serving with page-dattention. In *Proceedings of the 29th Symposium on Operating Systems Principles*, pages 611–626, 2023.
- [26] Taegyeong Lee, Zhiqi Lin, Saumay Pushp, Caihua Li, Yunxin Liu, Youngki Lee, Fengyuan Xu, Chenren Xu, Lintao Zhang, and Junehwa Song. Occlumency: Privacy-preserving remote deep-learning inference using sgx. In *The 25th Annual International Conference on Mobile Computing and Networking*, pages 1–17, 2019.
- [27] Dacheng Li, Rulin Shao, Hongyi Wang, Han Guo, Eric P Xing, and Hao Zhang. Mpcformer: fast, performant and private transformer inference with mpc. *arXiv preprint arXiv:2211.01452*, 2022.
- [28] Raymond Li, Loubna Ben Allal, Yangtian Zi, Niklas Muennighoff, Denis Kocetkov, Chenghao Mou, Marc Marone, Christopher Akiki, Jia Li, Jenny Chim, et al. Starcoder: may the source be with you! *arXiv preprint arXiv:2305.06161*, 2023.
- [29] Guo Lin, Wenyue Hua, and Yongfeng Zhang. Emojicrypt: Prompt encryption for secure communication with large language models. *arXiv preprint arXiv:2402.05868*, 2024.
- [30] Ji Lin, Jiaming Tang, Haotian Tang, Shang Yang, Weiming Chen, Wei-Chen Wang, Guangxuan Xiao, Xingyu Dang, Chuang Gan, and Song Han. Awq: Activation-aware weight quantization for llm compression and acceleration. In *MLSys*, 2024.
- [31] Xuanqi Liu and Zhuotao Liu. LLMs can understand encrypted prompt: Towards privacy-computing friendly transformers. *arXiv preprint arXiv:2305.18396*, 2023.
- [32] Natasha Lomas. Italy orders ChatGPT blocked citing data protection concerns. <https://techcrunch.com/2023/03/31/chatgpt-blocked-italy/>, 2023.
- [33] Ueli Maurer. Information-theoretic cryptography. In Michael Wiener, editor, *Advances in Cryptology — CRYPTO ’99*, volume 1666 of *Lecture Notes in Computer Science*, pages 47–64. Springer-Verlag, 8 1999.
- [34] Meta. Code Llama. <https://ai.meta.com/blog/code-llama-large-language-model-coding/>, 2024.
- [35] Meta. Llama 3. <https://llama.meta.com/llama3/>, 2024.
- [36] Maxim Milakov and Natalia Gimelshein. Online normalizer calculation for softmax. *arXiv preprint arXiv:1805.02867*, 2018.
- [37] Amachi Mitsu and Takahashi Yoshihide. Resume text classification dataset. *Kaggle competition*, 2021.
- [38] NBME. Score clinical patient notes. *Kaggle competition*, 2022.
- [39] Xuefei Ning, Zinan Lin, Zixuan Zhou, Huazhong Yang, and Yu Wang. Skeleton-of-thought: Large language models can do parallel decoding. *arXiv preprint arXiv:2307.15337*, 2023.
- [40] Nvidia. Nvidia confidential computing. <https://www.nvidia.com/en-us/data-center/solutions/confidential-computing/>, 2023.
- [41] Myle Ott, Sergey Edunov, Alexei Baevski, Angela Fan, Sam Gross, Nathan Ng, David Grangier, and Michael Auli. fairseq: A fast, extensible toolkit for sequence modeling. In Waleed Ammar, Annie Louis, and Nasrin Mostafazadeh, editors, *Proceedings of the 2019 Conference of the North American Chapter of the Association for Computational Linguistics: Human Language Technologies, NAACL-HLT 2019, Minneapolis, MN, USA, June 2-7, 2019, Demonstrations*, pages 48–53. Association for Computational Linguistics, 2019.
- [42] Ashwinee Panda, Tong Wu, Jiachen T Wang, and Prateek Mittal. Differentially private in-context learning. *arXiv preprint arXiv:2305.01639*, 2023.
- [43] Qi Pang, Jinhao Zhu, Helen Möllering, Wenting Zheng, and Thomas Schneider. Bolt: Privacy-preserving, accurate and efficient inference for transformers. In *2024 IEEE Symposium on Security and Privacy (SP)*, pages 4753–4771. IEEE, 2024.
- [44] Reiner Pope, Sholto Douglas, Aakanksha Chowdhery, Jacob Devlin, James Bradbury, Jonathan Heek, Kefan Xiao, Shivani Agrawal, and Jeff Dean. Efficiently scaling transformer inference. *Proceedings of Machine Learning and Systems*, 5:606–624, 2023.

- [45] Alec Radford, Jeffrey Wu, Rewon Child, David Luan, Dario Amodei, Ilya Sutskever, et al. Language models are unsupervised multitask learners. *OpenAI blog*, 1(8):9, 2019.
- [46] Siladitya Ray. Apple Joins A Growing List Of Companies Cracking Down On Use Of ChatGPT By Staffers—Here’s Why. <https://www.forbes.com/sites/siladityaray/2023/05/19/apple-joins-a-growing-list-of-companies-cracking-down-on-use-of-chatgpt-by-staffers-heres-why/?sh=49380e9628ff>, 2023.
- [47] Chris Renzo, Liv Aliberti, Justin Miles, and Joe Kovba. Large language model inference over confidential data using AWS Nitro Enclaves. <https://aws.amazon.com/blogs/machine-learning/large-language-model-inference-over-confidential-data-using-aws-nitro-enclaves/>, 2024.
- [48] Ronald L Rivest. Chaffing and winnowing: Confidentiality without encryption. *CryptoBytes (RSA laboratories)*, 4(1):12–17, 1998.
- [49] Mark Russinovich. Azure AI Confidential Inferencing: Technical Deep-Dive. <https://techcommunity.microsoft.com/t5/azure-confidential-computing/azure-ai-confidential-inferencing-technical-deep-dive/ba-p/4253150>, 2024.
- [50] Claude E Shannon. Communication theory of secrecy systems. *The Bell system technical journal*, 28(4):656–715, 1949.
- [51] Youren Shen, Hongliang Tian, Yu Chen, Kang Chen, Runji Wang, Yi Xu, Yubin Xia, and Shoumeng Yan. Occlum: Secure and efficient multitasking inside a single enclave of intel sgx. In *Proceedings of the Twenty-Fifth International Conference on Architectural Support for Programming Languages and Operating Systems*, pages 955–970, 2020.
- [52] Zhili Shen, Zihang Xi, Ying He, Wei Tong, Jingyu Hua, and Sheng Zhong. The fire thief is also the keeper: Balancing usability and privacy in prompts. *arXiv preprint arXiv:2406.14318*, 2024.
- [53] Mohammad Shoeybi, Mostofa Patwary, Raul Puri, Patrick LeGresley, Jared Casper, and Bryan Catanzaro. Megatron-lm: Training multi-billion parameter language models using model parallelism. *CoRR*, abs/1909.08053, 2019.
- [54] Xinyu Tang, Richard Shin, Huseyin A Inan, Andre Manoel, Fatemehsadat Mireshghallah, Zinan Lin, Sivakanth Gopi, Janardhan Kulkarni, and Robert Sim. Privacy-preserving in-context learning with differentially private few-shot generation. *arXiv preprint arXiv:2309.11765*, 2023.
- [55] Hugo Touvron, Thibaut Lavril, Gautier Izacard, Xavier Martinet, Marie-Anne Lachaux, Timothée Lacroix, Baptiste Rozière, Naman Goyal, Eric Hambro, Faisal Azhar, et al. Llama: Open and efficient foundation language models. *arXiv preprint arXiv:2302.13971*, 2023.
- [56] Ashish Vaswani, Noam Shazeer, Niki Parmar, Jakob Uszkoreit, Llion Jones, Aidan N Gomez, Łukasz Kaiser, and Illia Polosukhin. Attention is all you need. *Advances in neural information processing systems*, 30, 2017.
- [57] Wenhao Wang, Linke Song, Benshan Mei, Shuang Liu, Shijun Zhao, Shoumeng Yan, XiaoFeng Wang, Dan Meng, and Rui Hou. Nestedsgx: Bootstrapping trust to enclaves within confidential vms. *arXiv preprint arXiv:2402.11438*, 2024.
- [58] Thomas Wolf, Lysandre Debut, Victor Sanh, Julien Chaumond, Clement Delangue, Anthony Moi, Pierric Cistac, Tim Rault, Rémi Louf, Morgan Funtowicz, Joe Davison, Sam Shleifer, Patrick von Platen, Clara Ma, Yacine Jernite, Julien Plu, Canwen Xu, Teven Le Scao, Sylvain Gugger, Mariama Drame, Quentin Lhoest, and Alexander M. Rush. Transformers: State-of-the-art natural language processing. In *Proceedings of the 2020 Conference on Empirical Methods in Natural Language Processing: System Demonstrations*, pages 38–45, Online, October 2020. Association for Computational Linguistics.
- [59] Tong Wu, Ashwinee Panda, Jiachen T Wang, and Prateek Mittal. Privacy-preserving in-context learning for large language models. *arXiv preprint arXiv:2305.01639*, 2023.
- [60] Ziqian Zeng, Jianwei Wang, Junyao Yang, Zhengdong Lu, Huiping Zhuang, and Cen Chen. Privacyrestore: Privacy-preserving inference in large language models via privacy removal and restoration. *arXiv preprint arXiv:2406.01394*, 2024.
- [61] Shixuan Zhao, Mengyuan Li, Yinqian Zhangyz, and Zhiqiang Lin. vsgx: virtualizing sgx enclaves on amd sev. In *2022 IEEE Symposium on Security and Privacy (SP)*, pages 321–336. IEEE, 2022.

A Appendix

A.1 Proof of Theorem 4.1

Let $Q \in \mathbb{R}^d$ be the query vector. Partition the key and value matrices $K \in \mathbb{R}^{n \times d}$ and $V \in \mathbb{R}^{n \times d}$ into private and public components:

$$K = \begin{bmatrix} K_{\text{Pvt}} \\ K_{\text{Pub}} \end{bmatrix}, \quad V = \begin{bmatrix} V_{\text{Pvt}} \\ V_{\text{Pub}} \end{bmatrix}.$$

Compute the attention scores s by:

$$s = QK^\top = [QK_{\text{Pvt}}^\top \quad QK_{\text{Pub}}^\top] = [s_{\text{Pvt}} \quad s_{\text{Pub}}],$$

where $s_{\text{Pvt}} = QK_{\text{Pvt}}^\top$ and $s_{\text{Pub}} = QK_{\text{Pub}}^\top$. Define the softmax denominators:

$$\gamma = \sum_{i=1}^n \exp(s_i) = \gamma_{\text{Pvt}} + \gamma_{\text{Pub}},$$

with

$$\gamma_{\text{Pvt}} = \sum_{i=1}^{n_{\text{Pvt}}} \exp(s_{\text{Pvt},i}), \quad \gamma_{\text{Pub}} = \sum_{i=1}^{n_{\text{Pub}}} \exp(s_{\text{Pub},i}).$$

The attention output is:

$$\begin{aligned} \sigma(s)^\top V &= \sum_{i=1}^n \frac{\exp(s_i)}{\gamma} V_i \\ &= \frac{1}{\gamma} \left(\sum_{i=1}^{n_{\text{Pvt}}} \exp(s_{\text{Pvt},i}) V_{\text{Pvt},i} + \sum_{i=1}^{n_{\text{Pub}}} \exp(s_{\text{Pub},i}) V_{\text{Pub},i} \right) \\ &= \frac{\gamma_{\text{Pvt}}}{\gamma} \left(\frac{1}{\gamma_{\text{Pvt}}} \sum_{i=1}^{n_{\text{Pvt}}} \exp(s_{\text{Pvt},i}) V_{\text{Pvt},i} \right) \\ &\quad + \frac{\gamma_{\text{Pub}}}{\gamma} \left(\frac{1}{\gamma_{\text{Pub}}} \sum_{i=1}^{n_{\text{Pub}}} \exp(s_{\text{Pub},i}) V_{\text{Pub},i} \right) \\ &= \frac{\gamma_{\text{Pvt}}}{\gamma} \left(\sigma(s_{\text{Pvt}})^\top V_{\text{Pvt}} \right) + \frac{\gamma_{\text{Pub}}}{\gamma} \left(\sigma(s_{\text{Pub}})^\top V_{\text{Pub}} \right). \end{aligned} \tag{8}$$

Thus,

$$\begin{aligned} \sigma(QK^\top) V &= \frac{\gamma_{\text{Pvt}}}{\gamma_{\text{Pvt}} + \gamma_{\text{Pub}}} \sigma(QK_{\text{Pvt}}^\top) V_{\text{Pvt}} \\ &\quad + \frac{\gamma_{\text{Pub}}}{\gamma_{\text{Pvt}} + \gamma_{\text{Pub}}} \sigma(QK_{\text{Pub}}^\top) V_{\text{Pub}}, \end{aligned} \tag{9}$$

which completes the proof.

A.2 Proof of Theorem 5.2

To prove Theorem 5.2, we show that the two sets of subsequences are ϵ -close over \mathcal{D}_{LM} with Lemma A.1, and $(\epsilon + 2\Delta)$ -close over \mathcal{D} .

Lemma A.1. Let a_1, a_2, \dots, a_n and b_1, b_2, \dots, b_n be sequences where $0 \leq a_i, b_i \leq 1$. If $|a_i - b_i| < \epsilon/n$ for all i , then $|\prod_{i=1}^n a_i - \prod_{i=1}^n b_i| < \epsilon$.

Part I Let us denote each token in the subsequence S_{target} as random variables X_1, \dots, X_n , where X_1 is the start token and X_n is the end token. Let $f(X_i) = P(X_i | X_1, \dots, X_{i-1})$ be the conditional probability of token X_i , which is modeled by the language model LM , given the previous tokens and the context S . Similarly, we represent the tokens in a fake sequence sampled by GQS as Y_1, \dots, Y_n .

GQS partitions the next token distribution into $\frac{1}{\epsilon'}$ bins, where $\epsilon' = \epsilon/n$, and each bin contains tokens with probabilities within $[m\epsilon', (m+1)\epsilon']$, where m is the bin index. Since GQS samples Y_i from the same bin as X_i , it is true that $|f(X_i) - f(Y_i)| < \epsilon'$ for all i .

Finally, we can bound the difference between the probability of the target sequence, $\prod_{i=1}^n f(X_i)$, and the probability of the fake sequence, $\prod_{i=1}^n f(Y_i)$, as $n\epsilon' = \epsilon$, using Lemma A.1. That is,

$$\left| \prod_{i=1}^n f(X_i) - \prod_{i=1}^n f(Y_i) \right| < \epsilon$$

This is true for every pair of target and fake subsequences. Based on Definition 5.1, since the maximum difference between the probabilities (modeled by \mathcal{D}_{LM}) of any target and fake subsequences is ϵ , the two sets of subsequence are ϵ -close over \mathcal{D}_{LM} .

Part II Let us denote the subsequence S_{target} as s , and a fake n-gram sampled by GQS as s' . According to Part I and the definitions in §5.2, we have

$$\begin{aligned} |P_{\mathcal{D}}(s) - P_{\mathcal{D}}(s')| &= |P_{\mathcal{D}}(s) - P_{\mathcal{D}_{LM}}(s) + P_{\mathcal{D}_{LM}}(s) - P_{\mathcal{D}_{LM}}(s') \\ &\quad + P_{\mathcal{D}_{LM}}(s') - P_{\mathcal{D}}(s')| \\ &\leq |P_{\mathcal{D}}(s) - P_{\mathcal{D}_{LM}}(s)| + |P_{\mathcal{D}_{LM}}(s) - P_{\mathcal{D}_{LM}}(s')| \\ &\quad + |P_{\mathcal{D}_{LM}}(s') - P_{\mathcal{D}}(s')| \\ &\leq \epsilon + 2\Delta. \end{aligned}$$

This is true for every pair of target and fake subsequences. Based on Definition 5.1, since the maximum difference between the probabilities (modeled by \mathcal{D}) of any target and fake subsequences is $\epsilon + 2\Delta$, the two sets of subsequences are $(\epsilon + 2\Delta)$ -close over \mathcal{D} .

A.3 Example and Dataset Preparation for PO

For the evaluation of PO, we selected the initial 500 entries from clinical dialogue datasets and 1500 entries from USMLE Step 2 passages. Since the initial datasets were not tagged with PII information, we used ChatGPT to automatically tag HIPAA-sensitive information according to the guidelines from [20], along with its PII category. Each entry in these datasets averaged 13 redacted PII segments. An example of

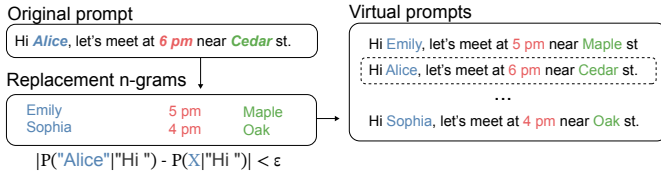


Figure 14: **PO example.** Given a prompt with its PII tagged (e.g., name and address), PO samples replacement tokens for each tagged token sequence using GQS. The generated fake tokens are statistically close to the original ones.

a dataset item is shown in Figure 15. For the resume dataset, we extracted the first 1500 entries and used Google Cloud’s PII filtering tool to annotate personal information, resulting in an average of 18 PII segments per entry. An anonymized example is presented in Figure 16.

Example Output from GQS. For demonstration, we present the result of running GQS on the name “Mrs. Loraine Wicks” in Figure 15, sampled with $\epsilon = 1/32$ and $\lambda_{\max} = 512$. Due to space constraints, only the first 30 outputs are shown.

	11. Mrs. Loraine Warner	21. Mrs. Lillian Winter
1. Mrs. Loraine Wicks	12. Mrs. Lydia Martin	22. Mrs. Lillian Abraham
2. Mrs. Lillian Brown	13. Mrs. Loraine Thompson	23. Mrs. Lillian Cooper
3. Mrs. Loraine Park	14. Mrs. Loraine Wood	24. Mrs. Lydia Davis
4. Mrs. Lydia Jackson	15. Mrs. Loraine Brown	25. Mrs. Lillian Kim
5. Mrs. Lydia Williams	16. Mrs. Lillian Grey	26. Mrs. Lillian Thompson
6. Mrs. Lillian Thomas	17. Mrs. Lillian Jenkins	27. Mrs. Lydia White
7. Mrs. Wilson	18. Mrs. Lillian Watson	28. Mrs. Lillian Davis
8. Mrs. Lydia Grant	19. Mrs. Lillian Anderson	29. Mrs. Lillian Carter
9. Mrs. Lillian Taylor	20. Mrs. Loraine Williams	30. Mrs. Loraine Miller
10. Mrs. Lydia Green		

A.4 Limitation of OSPD

Here, we discuss some limitations in OSPD as well as new opportunities.

When OSPD is impractical. In scenarios with only a few users but large workloads, the approach of serving entire LLM instances with per-user CVMs may be more practical. It is often the case for institutions or companies, a use case supported by several providers, such as OpenAI’s Foundry. In contrast, SPD enables efficient confidential prompting for a vast number of

end users, making it ideal for services that directly interact with large audiences, such as chatbots or personal assistants.

Integrity checks in SPD. One limitation of SPD is it assumes an HBC model because the CVM does not check the integrity of the received Q . For stronger threat models that do not assume adversaries will follow the protocol, integrity checking mechanisms on the received Q are necessary. For example, the CVM can partially retain the LLM weights in the TEE and use randomized algorithms, such as Freivalds’ algorithm, to check the integrity of the received Q without fully recomputing it, or implement a zero-knowledge protocol (ZKP).

[AGE] 17-year-old [GENDER] male, has come to the [ORGANIZATION NAME] student health clinic complaining of [DISEASE] heart pounding. [PERSON NAME] Mrs. Lorraine Wicks mother has given verbal consent for a history, physical examination, and treatment - began [DATES] 2-3 months ago, sudden, intermittent for [DATES] 2 days (lasting 3-4 min), worsening, non-allev/aggrav - associated with dyspnea on exertion and rest, stressed out about school - reports he feels like his heart is jumping out of his chest - ROS: denies chest pain, diaphoresis, weight loss, chills, fever, nausea, vomiting, pedal edema - PMH: none, meds: Adderall (from a friend), NKDA - FH: father had MI recently, mother has thyroid disease - SH: non-smoker, marijuana [DATES] 5-6 months ago, 3 beers on the weekend, basketball at school - SH: no STD.

Figure 15: Example entry from the clinical dataset. Yellow-masked text indicates redacted information, with brackets denoting its PII category.

Resume Wizard [PERSON NAME] Jane Doe E-Mail: [EMAIL] jane.doe@example.com Phone: [ID] (123) 456-7890 (M) [ORGANIZATION NAME] Finance & Accounts, Costing Profile Introduction

- A dynamic professional with a qualitative experience of [AGE] 3 years 2 months in the areas of Finance & Accounts, Product Costing & MIS Reporting.
- Presently working as PROCESS LEAD at [ORGANIZATION NAME] Tech Solutions Inc.
- Previously worked as LEAD F&A OPERATIONS at [ORGANIZATION NAME] Global Tech with [ORGANIZATION NAME] Soft Drinks Co Project from [DATES] 1st April 2018 to [DATES] 30th June 2019.
- Involved in the standardization of process & MIS reporting files and contributed a higher rate of organic growth.
- An effective communicator with excellent relationship-building & interpersonal skills. Strong analytical, problem-solving & organizational abilities.
- Areas of interest include budgeting & preparation of AOP (Annual Operating Plans).
- Familiar with SAP FICO modules, MS Office tools.

Figure 16: Example entry from the resume dataset. Note that we anonymized this example with placeholders such as “Jane Doe.” and “(123) 456-7890” for privacy.